PERIÓDICO TCHÊ QUÍMICA
ARTIGO ORIGINAL

AVALIAÇÃO DE EFICIÊNCIA DA DESPARAFINIZAÇÃO DE CALOR DO POÇO DE PRODUÇÃO EQUIPADA POR SUBBOMBA COM HASTES OCAS

EFFICIENCY EVALUATION OF THE HEAT DEPARAFINIZATION OF PRODUCING WELL EQUIPPED BY SUB PUMP WITH HOLLOW RODS

ОЦЕНКА ЭФФЕКТИВНОСТИ ПРОЦЕССА ТЕПЛОВОЙ ДЕПАРАФИНИЗАЦИИ СКВАЖИНЫ, ОБОРУДОВАННОЙ ГЛУБИННЫМ НАСОСОМ С ПОЛЫМИ ШТАНГАМИ

LEKOMTSEV, Alexander Viktorovich[1]*, KANG, Wanli [2], GALKIN, Sergey Vladislavovich[3], KETOVA, Yulia Anatolievna[4]

[1,3,4] Perm National Research Polytechnic University, Perm, Russian Federation

[2] School of Petroleum Engineering, China University of Petroleum (East China), Qingdao, China

*Corresponding author
e-mail: alex.lekomtsev@mail.ru

Received 24 August 2020; received in revised form 18 September 2020; accepted 22 October 2020

RESUMO

Uma das principais complicações da produção de petróleo é que os depósitos de asfalteno-resina-parafina (ARPD) são formados durante a operação dos poços de produção. Este é um problema urgente na indústria de petróleo e gás, especialmente nos campos da região de Ural-Volga (Rússia). Este estudo teve como objetivo desenvolver uma solução tecnológica para o tratamento térmico eficaz de depósitos a partir do cálculo do estado térmico dos poços durante o funcionamento de uma bomba de haste de sucção. Na prática, o efeito térmico no ARPD é realizado por lavagem com um agente quente (água, óleo). Tradicionalmente, as descargas são realizadas através do anular do revestimento. Porém, este método é ineficaz devido às grandes perdas de calor e à impossibilidade de aquecer de forma suficiente a parte interna da tubulação, onde o ARPD é depositado. A modelagem dinâmica do processo foi realizada no produto de software ANSYS Fluent. O problema do calor foi resolvido com base na equação de transferência média de calor e massa de Navier-Stokes Reynolds. Observou-se que a temperatura do agente injetado (óleo quente ou água) afeta a temperatura da parede interna da tubulação em menor grau do que a vazão do refrigerante. Foi estabelecido que é impossível atingir o ponto de fusão da cera no nível da bomba submersível. A taxa de fluxo do refrigerante afeta este parâmetro mais intensamente. Ao lavar com óleo quente a 120°C com vazão de 300 m^3/dia, a temperatura acima da bomba será igual à temperatura de derretimento da cera. Os cálculos indicam que é mais aconselhável usar óleo aquecido a 120°C como refrigerante para a lavagem de poços do que água com temperatura de 90°C. A implementação do método proposto pode ser usado em qualquer poço equipado com uma bomba de haste de sucção

Palavras-chave: *complications at oil-producing, hollow rods, flushing-out of well.*

ABSTRACT

One of the main oil production complications is that asphaltene-resin-paraffin deposits (ARPD) are formed during production wells' operation. This is an urgent problem in the oil and gas industry, especially in the fields of the Ural-Volga region (Russia). This study aimed to develop a technological solution for the effective thermal treatment of deposits based on the wells' thermal state calculation during a sucker rod pump operation. In practice, the thermal effect on ARPD is carried out by flushing-out with a hot agent (water, oil). Traditionally, flushes are carried out through the casing annulus. However, this method is ineffective due to large heat losses and the impossibility of heating the inner part of the tubing in a sufficient way, where ARPD is deposited. Dynamic modeling of the process was performed in the ANSYS Fluent software product. The heat problem was solved on the basis of the Navier-Stokes Reynolds-averaged heat and mass transfer equation. It was noted that the temperature of the injected agent (hot oil or water) affects the temperature of the tubing's inner wall to a lesser extent than the coolant flow rate. It has been established that it is impossible to reach the melting point of wax at the submersible pump level. The flow rate of the coolant affects this parameter more intensively. When flushing with hot oil 120°C with a flow rate of 300 m^3/day, the temperature above the pump will be equal to the wax melting temperature. Calculations indicate that it is most advisable to use oil heated to 120°C as a coolant for flushing

DOI: 10.52571/PTQ.v17.n36.2020.765_Periodico36_pgs_750_765.pdf

wells than water with a 90°C temperature. The implementation of the methods proposed can be used on any well equipped with a sucker rod pump.

Keywords: *complications at oil-producing, hollow rods, flushing-out of well.*

АННОТАЦИЯ

Одним из основных осложнений при добыче нефти является образование асфальтеносмолопарафинистых отложений (АСПО) при эксплуатации добывающих скважин. Это актуальная проблема в нефтегазовой отрасли, особенно на месторождениях Урало-Поволжья (Россия). Целью данной работы являлась разработка технологического решения для эффективного воздействия термическим методом на отложения на основе расчета теплового состояния скважин во время работы штангового глубинного насоса. На практике термическое воздействие на АСПО осуществляется путем промывки горячим агентом (вода, нефть). Традиционно промывки проводят через затрубное пространство. Однако такой способ неэффективен за счет больших потерь тепла и невозможности прогрева внутренней части насосно-компрессорных труб (НКТ), где откладывается АСПО, достаточным образом. Динамическое моделирование процесса проводилось в программном продукте ANSYS Fluent. Тепловая задача решалась на основе уравнения тепломассопереноса, усредненного по Навье-Стоксу и Рейнольдсу. Было отмечено, что температура нагнетаемого агента (горячей нефти или воды) влияет на температуру внутренней стенки НКТ в меньшей степени, чем скорость потока теплоносителя. Установлено, что достичь точки плавления АСПО на уровне погружного насоса невозможно. Расход теплоносителя сильнее влияет на этот параметр. При промывке горячей нефтью при 120°C с расходом 300 м3/сут температура над насосом будет равна температуре плавления парафина. Расчеты показывают, что в качестве теплоносителя для промывки скважин целесообразнее использовать нагретую до 120°C нефть, чем воду с температурой 90°C. Предложенный метод может быть использован на любой скважине, оборудованной штанговым насосом.

Ключевые слова: *осложнения при добыче нефти, полые штанги, промывки скважин*

1. INTRODUCTION:

Within the territory of the Perm region, the main problem arising during the operation of wells is asphaltene-resin-paraffin deposits (ARPD), establishing onto the surface of deep-pumping equipment (Figure 1) (Khizhnyak, 2014). Wherein, there are premature failures of pumping equipment and well shutdowns, accompanied by shortages in oil production (Eskin, 2014). Known methods for paraffin deposition prognostication are divided into two main groups – methods aimed to determine the depth of the beginning of ARPD establishing (the beginning of paraffin crystallization) and methods determining the intensity (velocity) of ARPD establishing (Johansen, 1991; Newberry, 1999; Turbakov, 2009; Escobedo, 2010; Aiyejina, 2011; Al-Yaari, 2011).

The basis for determining the depth of the beginning of the formation of paraffin deposits are the physical and chemical properties of oil and thermodynamic conditions of its production (Korobov, 2018; Movchan *et al*., 2019). As the oil lifts through the pipe, the flow's temperature and pressure decrease to the paraffin-formation point (Rehan, 2016; Sullivan, 2020; Abramovich *et al*., 2019). Above this deep, ARPD is sedimented on the pipe surfaces and equipment plugging free space. The interval of intensive deposits is 300-800 m for the Ural-Volga fields.

There are thermal, chemical, and mechanical ways among different methods of ARPD removing from well (Huang, 2016; Wang, 2015). The simple-to-apply method is mechanical, but there is a risk of jamming rods and equipment failure when the process of paraffin deposition is quite intensive. The chemical method is expensive when chemicals are required in a lot rate (Hassan, 2019). The thermal method has industrial limitations about heating agents and transporting it to wells (Zhao, 2015). But the choice of technological and economic effective method depends on the content of paraffin, resin and asphaltenes (Buenrostro-Gonzalez, 2004; Bemani, 2019). In practice, the intensity of precipitation of solid organic substances is estimated using the inter-cleaning period (ICP) of the well (Moradi, 2019), which means the interval between cleaning. The ICP is evaluated practically and set in such a way when producing wells work without failures connected with ARPD. Flushing of wells is the most economically and technologically method in condition with low ICP and intensive organic deposits (Barker, 1999; Ustkachkintsev, 2016; Mahmoud, 2019). It has current interest when deposits have stable surface crust from asphaltene-wax complexes (Rogel, 2015), which leads to a decrease in their solubility by chemical

(Zlobin, 2015; Hashemi, 2016; Guzman, 2017; Khalaf, 2019; Behnous, 2020).

Hot oil and freshwater are considered to be coolant (agent). These are traditional agents, which are found in the oil treatment plant and easy to get at any time. Typically, such an agent can be delivered to the well site within 1 or 2 hours by special trucks.

Therefore, this study aimed to develop a technological solution for the effective thermal treatment of deposits based on the calculation of the wells' thermal state during a sucker rod pump operation.

2. MATERIALS AND METHODS:

In this study, there were considered wells equipped with sucker rod pumps (SRP), artificial-lift pumping systems. The system has a surface power source to drive a downhole pump assembly. A beam and crank assembly create reciprocating motion in a sucker-rod string that connects to the downhole pump assembly. The pump contains a plunger and valve assembly to convert the reciprocating motion to vertical fluid movement. The authors deal with a topical issue of conducting thermal treatment throughout the SRP's hollow rods without shutting a well-operating down. Currently, the theoretical material and field experience of wells backwash with coolant supply into the annular space (Ramey, 2013) have been accumulated, but systematic ideas concerning the effectiveness of flushing throughout hollow rods have not been represented (Garcia, 2001; Soulgani, 2010; Khaleel, 2020; Kovalev, 2018; Yemelyanov *et al*., 2019).

The issue regarding estimation of a thermal condition of a well under the heat treatment throughout hollow rods and the definition of the most optimal conditions concerning effective removal of ARPD was considered.

2.1. Problem Statement and Solution

The geometric model of a well is shown in Figure 2. SRP is lowered onto the tubing into the well. The movement of the pump plunger is performed throughout the hollow rods. A coupling is installed to bypass the coolant from the rod column into the tubing at a given depth. During the well's operation, the coolant is fed into the hollow rods, passing through which, the agent heats the flow of downhole products, leaves through the coupling, then are mixed with the main flow and rise to the wellhead. An essential advantage of this technology before flushing the well throughout the annular space is reducing heat losses into the environment, thereby increasing heat flow density into the ARPD removal area.

The main tasks were to determine the coolant's temperature at which the complete melting of paraffin occurs and assess the impact of operational characteristics of the well regarding the washing efficiency.

2.2. Method of Solving Problem

The stated problems were solved numerically by the finite element method. The finite element method is a systematic way to convert the functions in an infinite-dimensional function space to the first function in finite-dimensional function space. Finally, ordinary vectors (in a vector space) tractable with numerical methods. It used the realizable k-epsilon (k-e) model as a model of turbulent heat-and-mass transfer Reynolds-Averaged Navier-Stokes (RANS) (Launder, 1972; Wilcox, 1998; Sumer, 2007). The traditional RANS equations are directly applied for turbulent flow and heat transfer of the fluid, ignoring the thermal physical properties' turbulent effect due to the intense nonlinearity.

This model was relatively recently developed. It differs from the standard k-e model by (Shih, 1995; Dobek, 2012) (1) improving notation for turbulent viscosity; and (2) the new transport equation for the dissipation rate is obtained from the exact transport equation for the mean-square pulsating vortex. The realizable k-e model was tested for the case of a single rotating coordinate system. The results showed a more accurate solution than in the case of the standard k-e turbulence model. Used in the article model describes well sufficiently for a round section modeling pipe.

The interaction of well production and coolant was described by the convection-diffusion equation (Jia, 2014). The natural convection was considered within the paper. The issue was solved as stationary (Lei, 2016). The thermophysical properties of solid materials did not depend on temperature. A limited area replaced the infinite array of the earth. The oil liquid was considered a single-phase medium (Ghasemi, 2020). The axisymmetric formulation of the issue was used to save computing resources (Table 1). The ICEM CFD processor was used to construct a geometric model. It divided the model into a finite element mesh (Figure 3). Engineering calculations were performed in the software product ANSYS Fluent.

2.3. Numerical experiment

The mathematical model of motion and heat transfer within an oil well is based on the rules of conservation of mass, amount of motion, and energy (Shirani, 2012; Al-Safran, 2018). Taking into account the assumptions made, the system of differential equations has got the form (1)-(9). Transfer equations (Navier-Stokes equations averaged by Reynolds):

$$\rho_i(\bar{\upsilon}_{ir}\frac{\partial\bar{\upsilon}_{ir}}{\partial r}+\bar{\upsilon}_{iz}\frac{\partial\bar{\upsilon}_{ir}}{\partial z})= =-\frac{\partial\bar{P}_i}{\partial r}+\mu_i\left(\frac{\partial^2\bar{\upsilon}_{ir}}{\partial r^2}+\frac{1}{r}\frac{\partial\bar{\upsilon}_{ir}}{\partial r}+\frac{\partial^2\bar{\upsilon}_{ir}}{\partial z^2}-\frac{\bar{\upsilon}_{ir}}{r^2}\right)+ +\frac{1}{r}\frac{\partial}{\partial r}\left(-r\rho_i\overline{\upsilon_{ir}'^2}\right)+\frac{\partial}{\partial z}\left(-\rho_i\overline{\upsilon_{ir}'\upsilon_{iz}'}\right), \quad (1)$$

$$\rho_i(\bar{\upsilon}_{ir}\frac{\partial\bar{\upsilon}_{iz}}{\partial r}+\bar{\upsilon}_{iz}\frac{\partial\bar{\upsilon}_{iz}}{\partial z})= =-\frac{\partial\bar{P}_i}{\partial z}+\mu_i\left(\frac{\partial^2\bar{\upsilon}_{iz}}{\partial r^2}+\frac{1}{r}\frac{\partial\bar{\upsilon}_{iz}}{\partial r}+\frac{\partial^2\bar{\upsilon}_{iz}}{\partial z^2}\right)+ +\frac{1}{r}\frac{\partial}{\partial r}\left(-r\rho_i\overline{\upsilon_{ir}'\upsilon_{iz}'}\right)+\frac{\partial}{\partial z}\left(-\rho_i\overline{\upsilon_{iz}'^2}\right), \quad (2)$$

Transporting equation for the kinetic energy of turbulence k :

$$(\frac{\partial\rho_i k\bar{\upsilon}_{ir}}{\partial r}+\frac{\partial\rho_i k\bar{\upsilon}_{iz}}{\partial z})=\frac{\partial}{\partial r}\left[\left(\mu_i+\frac{\mu_t}{\sigma_k}\right)\frac{\partial k}{\partial r}\right]+ +\frac{\partial}{\partial z}\left[\left(\mu_i+\frac{\mu_t}{\sigma_k}\right)\frac{\partial k}{\partial z}\right]+G_k+G_b-\rho_i\varepsilon-Y_M \quad (3)$$

(3)

Transfer equation for the rate of dissipation of the kinetic energy of turbulence:

$$(\frac{\partial\rho_i\varepsilon\bar{\upsilon}_{ir}}{\partial r}+\frac{\partial\rho_i\varepsilon\bar{\upsilon}_{iz}}{\partial z})=\frac{\partial}{\partial r}\left[\left(\mu_i+\frac{\mu_t}{\sigma_\varepsilon}\right)\frac{\partial\varepsilon}{\partial r}\right]+ +\frac{\partial}{\partial z}\left[\left(\mu_i+\frac{\mu_t}{\sigma_\varepsilon}\right)\frac{\partial\varepsilon}{\partial z}\right]+\rho_i C_1 S\varepsilon- -\rho_i C_2\frac{\varepsilon^2}{k+\sqrt{\nu_i\varepsilon}}+C_{1\varepsilon}\frac{\varepsilon}{k}C_{3\varepsilon}G_b \quad (4)$$

Turbulent viscosity μ_t :

$$\mu_t=\rho_i C_\mu\frac{k^2}{\varepsilon} \quad (5)$$

Continuity equation:

$$-\rho_i\left(\frac{\partial\left(r\bar{\upsilon}_{iz}\right)}{\partial z}+\frac{\partial\left(r\bar{\upsilon}_{ir}\right)}{\partial r}\right)= =\left(\bar{\upsilon}_{iz}\frac{\partial\left(r\rho_i\right)}{\partial z}+\bar{\upsilon}_{ir}\frac{\partial\left(r\rho_i\right)}{\partial r}\right) \quad (6)$$

Energy equation:

$$\frac{\partial}{\partial r}\left[\bar{\upsilon}_{ir}\left(\rho_i E+p\right)\right]+\frac{\partial}{\partial z}\left[\bar{\upsilon}_{iz}\left(\rho_i E+p\right)\right]= =\frac{\partial}{\partial r}\left(k_{eff}\frac{\partial T}{\partial r}+\bar{\upsilon}_{ir}\left(\tau\right)_{eff}\right)+ +\frac{\partial}{\partial z}\left(k_{eff}\frac{\partial T}{\partial z}+\bar{\upsilon}_{iz}\left(\tau\right)_{eff}\right)+S_h \quad (7)$$

Convection-diffusion equation:

$$\frac{\partial(\rho_i\vec{v}Y_i)}{\partial r}+\frac{\partial(\rho_i\vec{v}Y_i)}{\partial z}= =-\left(\frac{\partial\vec{J}_i}{\partial r}+\frac{\partial\vec{J}_i}{\partial z}\right)+R_i+S_i \quad (8)$$

where $\vec{J}_i$- is the diffusion flow, which is as:

$$\vec{J}_i=-\left(\rho_i D_{i,m}+\frac{\mu_t}{Sc_t}\right)\left(\frac{\partial Y_i}{\partial r}+\frac{\partial Y_i}{\partial z}\right)- -D_{T,i}\frac{\nabla T}{T} \quad (9)$$

where r, z - cylindrical coordinates; i - index of areas studied, i=1- oil, i=2 -associated petroleum gas, i=3- pump - compressor- pipe, i=4- casing

string, *i=5* -hollow rods, *i=6*- soil; *i=7*- water; $\bar{\upsilon}_{ir}\bar{\upsilon}_{iz}$- time - averaged velocity components; $\upsilon'_{ir}\upsilon'_{iz}$- pulsation velocity components;$\overline{\upsilon'_{ir}\upsilon'_{iz}}$- turbulent stresses; T-temperature;$\bar{P}_i$- time-averaged pressure; ρ_i-medium density; μ_i- dynamic viscosity of the medium; k-kinetic energy of turbulence; ε-velocity turbulence energy dissipation;σ_k and σ_ε- turbulent Prandtl numbers for $k$and ε, respectively; G_k-kinetic energy of turbulence due to mean velocity gradients;G_b - kinetic energy of turbulence due to buoyancy; μ_t-turbulent viscosity; C_μ-variable determining turbulent viscosity; ν_i-kinematic viscosity; Y_M-dilation dissipation taking into account the effect of compressibility under turbulence; C_2,$C_{1\varepsilon}$,$C_{3\varepsilon}$- constants; E-total energy; $(\tau)_{eff}$-deviator stress tensor; k_{eff}-effective thermal conductivity; S_h-volumetric heat sources; Y_i-mass fraction of substance; $\vec{J}_i$-diffusion flux; R_i-reaction rate; S_i-mixing rate with dispersed phase; $D_{i,m}$-mass diffusion coefficient; Sc_t-Schmidt turbulent number; $D_{T,i}$-turbulent diffusion, - author defined source; $\vec{\nu}$ - molecular kinetic viscosity; *p* - pressure.

During the numerical experiment, the following characteristics of the deep-pumping equipment were taken as initial data: the diameter and wall thickness of casing – 146 mm and 8 mm; the tubing diameter and wall thickness – 73 and 5.5 mm; the length, diameter, and wall thickness of the 1st stage rod string is 500 m, and 4 37 mm; the length, diameter and wall thickness of the 2nd stage rod string – 300 m, 34th and 3.5 mm; the installation depth of the by-pass coupling (H_{coup}) – 800 m; the temperature of the downhole production installation depth of clutch – 15 °C; geothermal gradient is 0.02 deg/m; the melting point of the paraffin – 52 °C (at the wellhead), 60 °C (level of coupling) (Turbakov, 2011); the production rate of oil of 20 m^3/day. Thermophysical characteristics of materials and media are provided in Table 2.

2.4. Practical Substantiation

To assess the possibility of ARPD removing (melting) within the tubing under heat treatment throughout hollow rods, a temperature distribution (onto the tubing inner wall (products extracted within the wellbore) is defined depending on the flow rate and the temperature of the coolant of 120, 200, 300°C. The temperature of 200 and 300°C is adopted to perform theoretical calculations and evaluate heat treatment possibilities.

To confirm the applicability of the results, the hydraulic resistance was evaluated during the organization of heat treatments through hollow rods. Further calculations were carried out, considering the volume and duration of time, based on flushing wells' practical experience. The results of such operations onto wells within the Ural-Volga region indicate the practical applicability and definite success of the operation with a flow rate of 12-16 m^3 / h (288-384 m^3/day) using a well dewaxing unit (ADP, ADPM type) without additional pumping equipment.

Besides, upon injecting the coolant into the well throughout the hollow rods, the inevitable pressure loss to overcome the hydrodynamic resistances occurs. The estimation of the pressure loss onto the resistances during the motion of the coolant was performed according to the Darcy-Weisbach equation:

$$\mathrm{P}_r = \lambda \frac{L}{d} \frac{V^2}{2} \rho \qquad (10)$$

where *λ* – the coefficient of hydraulic resistance based onto the flow mode (turbulent and laminar), and the value of the Reynolds number per this high-speed flow regime, *Re=f(V, d, v); L* – characteristic length; *d* – characteristic outer diametre, *V* – the linear flow velocity; *ρ, v* – the density and kinematic viscosity of the coolant.

3. RESULTS AND DISCUSSION:

The calculations for oil and water washing for the flow rate of 300 m^3/day and the problem's conditions are shown in Tables 3 and 4. Using the equivalent roughness value within the range of 0.15-0.3 mm, which corresponds to the values for pipes past several years of operation, the total pressure loss according to The Altschul formula $\lambda=0.11\ (\Delta/d)^{0.25}$ was 13.2-15.7 MPa (*Δ* - equivalent absolute roughness). The estimated calculations regarding the determination of hydraulic resistances associated with the loss of pressure due to friction forces along the rod column's length also confirm the applicability under specified conditions, only within the range of costs up to 300m^3/day with the involvement of ADP without additional equipment. The pressure loss during the agent's delivery into the coupling inlet to a depth of 800 m does not exceed 16 MPa within this flow range.

Figure 4 displays that even at the injected hot oil temperature equal to 300ºC (curve 1), the temperature at the coupling level falls below the

paraffin's melting point and is 47ºC. While at a coolant temperature equal to 120ºC, the coupling inlet's temperature is 36ºC (curve 3). According to the calculation results, it may be noted that the coolant's temperature has got its little effect on the temperature of the inner wall of the tubing at a depth of 800 meters. By changing this parameter within the technical capabilities of oilfield equipment (not above 150ºC), it is not possible to achieve effective well heating.

The agent's thermal power injected for warming up the well is determined by its temperature and thermophysical properties and the flow rate. Therefore, to assess this parameter's influence, the problems for the coolant injection conditions of 150, 250, and 300 m^3/day, respectively, are solved. The results are shown in Figure 5. Upon increasing the coolant flow rate, the tubing's inner wall's temperature at the coupling level increases more significantly compared to the increase in the coolant temperature (Figure 5). When oil heated up to 120°C is pumped at a flow rate of 300 m^3 / day, the temperature at the coupling level is 59-60°C, which corresponds to the melting point of paraffin (Figure 5). Therefore, within the entire considered area, the wax will melt. At the same flow rates, when the water plays the role of the coolant being heated up to 90ºC, the temperature equal to the melting temperature of paraffin is not reached at the level of the coupling (Figure 6).

Under these technological parameters of production, changing the coolant's temperature, it is not possible to achieve the temperature at the level of the coupling equal to the melting temperature of paraffin. Technologically, it is more efficient to change the flow rate of the coolant. Thus, under the oil temperature equal to 120°C and a flow rate of 300 m^3/day, the temperature at the coupling inlet is equal to paraffin's melting temperature.

The degree of heating of downhole products during thermal washing throughout hollow rods depends on the well's technological mode of operation. The value of the dynamic liquid level within the annular space (H_{dyn}) has got its significant impact. Upon increasing the H_{dyn}, the petroleum-associated gas column height increases, removing the heat to the surrounding rocks less intensively than the liquid column. For operating conditions of wells within the Perm region, the dynamic level is maintained at 150-300 m above the depth of the rod pump descent, which is, on average, 900-1200 m (Kamentschikov, 2005).

The well model can also be divided into zones reflecting the dewaxing process stages performed by pumping coolant within the volume of 150 m^3/day into hollow rods located in the tubing (Jorg Oschrmann, 2002). In zone I the temperature onto the tubing wall does not fall below 52ºC; therefore, it may be argued that there is a complete melting of paraffin within this area. In zone II the exfoliation of paraffin deposits is most likely. This zone's lower boundary is determined by the temperature at which the paraffin mass shift is observed (30-32ºC) (Zlobin, 2015). In zone III, the zone of weakened adhesion of paraffin to the surface of the pipe is very small and is assumed to be 50 m; and in zone IV is practically inaccessible for the method of thermal dewaxing of wells.

Figure 7 depicts an example of the calculations' results regarding the area of probable (I-III) ARPD washing out. The calculations of the probable depth of the ARPD washing out were made regarding the conditions of washing with hot water and oil under different dynamic liquid levels within the annular space. The results are shown in Table 5. In this theoretical research, the effectiveness evaluation method is used to study the effect of ARPD removal and application study results to the real industry (Kamentschikov, 2005; Rahman, 2017). This section discusses the interpretation of modeling results during the process of flushing out of wells.

4. CONCLUSIONS:

It can be concluded that, as the coolant for flushing-out of well, it is most expedient to use oil heated up to 120°C than water with its temperature of 90 ° C. The best indicators of the technological efficiency of the flushing-out of well with the coolant are observed provided that $H_{dyn}>H_{coup}$, and with the increase in the dynamic level in the well, the thermal efficiency washing throughout the hollow rods is increased. It was established that, given the technological production parameters and the increase of the coolant temperature, it is not possible to reach the melting point of the paraffin at the depth of the coupling level. The flow rate of the coolant affects this parameter more intensively. Thus, under the oil temperature equal to 120°C and a flow rate of 300 m^3/day, the temperature at the coupling inlet is equal to paraffin's melting temperature. Improving the technological efficiency of the technology of washing wells throughout hollow rods may enhance the design of the rod column and its coating with thermal insulation materials.

5. ACKNOWLEDGMENTS:

The article was prepared based on research conducted with financial support from the Russian Ministry of Education and Science within the framework of the Federal Target Program “Research and Development in Priority Directions for the Development of the Russian Science and Technology Complex for 2014–2020” (Unique project identifier RFMEFI62120X0038.)

6. REFERENCES:

1. Aiyejina, A, Chakrabarti, D.P., Pilgrim, A., and Sastry, Mk. S. (2011). Wax formation in oil pipelines: A critical review. *International journal of multiphase flow,* 7, 671-694. https://doi.org/10.1016/j.ijmultiphaseflow.2011.02.007
2. Abramovich, B. N., Sychev, Y. A., and Zimin, R. Y. (2019). Efficiency estimation of hybrid electrical complex for voltage and current waveform correction in power systems of oil enterprises. Paper presented at the *Proceedings of the 2019 IEEE Conference of Russian Young Researchers in Electrical and Electronic Engineering, ElConRus 2019,* 401-406. https://doi:10.1109/EIConRus.2019.8657081
3. Al-Safran, E., (2018). Prediction of asphaltene precipitation risk in oil wells using coupled thermohydraulics model. *Journal of Petroleum Science and Engineering*, 167, 329-342. https://doi.org/10.1016/j.petrol.2018.04.024
4. Al-Yaari, M. (2011). Paraffin wax deposition: Mitigation and removal techniques. *Proceedings of the SPE Saudi Arabia Section Young Professionals Technical Symposium,* 14-16. https://doi.org/10.2118/155412-MS
5. Barker, K.M., Sharum, D.B, and Brewer, D. (1999). Paraffin damage in high temperature formations, removal and inhibition. SPE 52156-MS. *The 1999 SPE Mid-Continent Operations Symposium, Oklahoma City, Oklahoma*, 28 – 31.
6. Behnous, D., Palma, A., Zeraibi, N., and Coutinho, J.A. (2020). Modeling asphaltene precipitation in Algerian oilfields with the CPA EoS. *Journal of Petroleum Science and Engineering,* 190, 107-115. https://doi.org/10.1016/j.petrol.2020.107115
7. Bemani, A., Poozesh, A., Bahrami M., and Ashoori, S., (2019). Experimental study of asphaltene deposition: Focus on critical size and temperature effect. *Journal of Petroleum Science and Engineering*, 181, 106-186 https://doi.org/10.1016/j.petrol.2019.106186
8. Buenrostro-Gonzalez, E., Lira-Galeana, C., Gil-Villegas, A. Wu J. (2004). Asphaltene precipitation in crude oils: Theory and experiments. *AIChE Journal*, 50 (10), 2552-2570. https://doi.org/10.1002/aic.10243
9. Dobek, S. (2012). Fluid dynamics and the Navier – Stokes Equation, available at: http://www.cs.umd.edu/~mount/Indep/Steven_Dobek/dobek-stable-fluid-final-2012.pdf
10. Garcia, M., and Carbognani, L. (2001). Asphaltene-paraffin structural interactions. Effect on crude oil stability. *Energy and Fuels*, 15 (05), 1021–1027. https://doi.org/10.1021/ef0100303
11. Ghasemi, M., and Al-Safran E. (2020). Integrated reservoir/wellbore production model for oil field asphaltene deposition management. *Journal of Petroleum Science and Engineering*, 192, 107-213. https://doi.org/10.2523/IPTC-19936-MS
12. Guzman, R, Ancheyta, J, Trejo, F, and Rodriguez, S. (2017). Methods for determining asphaltene stability in crude oils. *Fuel*, 188, 530–543. https://doi.org/10.1016/j.fuel.2016.10.012
13. Escobedo, J., and Mansoori, G. A. (2010). Heavy-organic particle deposition from petroleum fluid flow in oil wells and pipelines. *Pet. Sci.*, 7, 502–508. https://doi.org/10.1007/s12182-010-0099-4
14. Eskin, D, Ratulowski, J., and Akbarzadeh, K. (2014). Modelling wax deposition in oil transport pipelines. *The Canadian Journal of Chemical Engineering 92(6).* https://doi.org/10.1002/cjce.21991
15. Hassan, A. Alade, O. Mahmoud, and M. Al-Majed, A. (2019). A Novel Technique for Removing Wax Deposition in the Production System Using

Thermochemical Fluids. *Abu Dhabi International Petroleum Exhibition and Conference, 11-14 November, Abu Dhabi, UAE.* https://doi.org/10.2118/197323-MS

16. Hashemi, R., Kshirsagar, L.K., Jadhav, P.B., Nandi, S., and Ghaleh, E. (2016). An overview on asphaltene precipitation phenomena from crude oil. *International Journal of Chemical Studies,* 4 (02), 46–50.
17. Huang, Q., Wang, W., Li, W., Ren Y., and Zhu F., (2016) A Pigging Model for Wax Removal in Pipes, *SPE Annual Technical Conference and Exhibition, 26-28 September, Dubai, UAE.* https://doi.org/10.2118/181560-MS
18. Jia, R., Wang, Y., Xiong, J., and Shi, H. (2014). Experimental and numerical study on the self-balancing heating performance of a thermosyphon during the process of oil production. *Applied Thermal Engineering*, 73 (1), 1270-1278. https://doi.org/10.1016/j.applthermaleng.2014.09.027
19. Johansen, S T. (1991). The deposition of particles on vertical walls. *International Journal of Multiphase flow*, 3, 355–362. https://doi.org/10.1016/0301-9322(91)90005-N
20. Jorg Oschrmann, H., (2002). New methods for the selection of asphaltenes inhibitors in the field. *Chemistry in the oil industry,* 254-255. https://doi.org/10.1039/9781847550460-00254
21. Kamentschikov, F. A. (2005). The Thermal Dewaxing of Wells. *M. Izhevsk: SRC "Regular and Chaotic Dynamics"*, 253.
22. Khalaf, M. H., Mansoori G. A., Yong, and Ch. W. (2019). Magnetic treatment of petroleum and its relation with asphaltene aggregation onset (an atomistic investigation). *Journal of Petroleum Science and Engineering*, 176, 926-933. https://doi.org/10.1016/j.petrol.2019.01.059
23. Khaleel, A.T., Abutaqiya, M.I.L., Sisco, C.J., and Vargasa, F.M. (2020). Mitigation of asphaltene deposition by re-injection of dead oil*. Fluid Phase Equilibria*, 514, 112-143. https://doi.org/10.1016/j.fluid.2020.112552
24. Khizhnyak, G. P., Usenkov, A.V., and Ustkachkintsev, E. N. (2014). Complicating Factors in the Development of the Nozhov Group of Deposits of "LUKOIL-PERM" LLC. *Vestnik permskogo natsional'nogo issledovatel'skogo politekhnicheskogo universiteta. Geologiya. neftegazovoe i gornoe delo (the Bulletin of Perm National Research Polytechnic University. Geology. Oil, Gas and Mining*), 13, 59-68. (in Russ).
25. Korobov, G., and Podoprigora, D. (2018). Depth computation for the onset of organic sedimentation formation in the oil producing well as exemplified by the Sibirskoye oil field. *Acta Technica CSAV (Ceskoslovensk Akademie Ved) 63(3),* 481-492. http://www.actatechnica.com/63(2018)-3/Complete%20Issue%2063(2018)-3.pdf
26. Kovalev, A.V. Miftakhov, R. T. Ryakhin, M. S. and Kolyvanov, A. V. (2018). Equipment for flushing of wells complicated by asphaltene-resin-paraffin deposits using hollow sucker rods. *Oil Industry Journal, (07).* https://doi.org/10.24887/0028-2448-2018-7-110-112
27. Launder B.E., and Spalding D.B. (1972). Lectures in Mathematical Models of Turbulence. *London, Academic Press*, 169. https://doi.org/10.1016/0307-904X(86)90045-4
28. Lei, Y., Han, Sh., and Zhang, J., (2016). Effect of the dispersion degree of asphaltene on wax deposition in crude oil under static conditions. *Fuel Processing Technology*, 146, 20-28. https://doi.org/10.1016/j.fuproc.2016.02.005
29. Mahmoud, M., (2019). Well Clean-Up Using a Combined Thermochemical /Chelating Agent Fluids. *Journal of Energy Resources Technology, 141(10), p.102905*. https://doi.org/10.1115/1.4043612
30. Moradi, S., Amirjahadi S., Danaee I., and Soltanic B., (2019). Experimental investigation on application of industrial coatings for prevention of asphaltene deposition in the well-string. *Journal of Petroleum Science and Engineering*, 181, 106-195.

https://doi.org/10.1021/acs.energyfuels.5b01237

31. Movchan, I. B., Yakovleva, A. A., and Daniliev, S. M. (2019). Parametric decoding and approximated estimations in engineering geophysics with the localization of seismic risk zones on the example of northern part of kola peninsula. *Paper presented at the 15th Conference and Exhibition Engineering and Mining Geophysics 2019*, Gelendzhik 2019, 188-198. https://doi:10.3997/2214-4609.201901705

32. Newberry, M. E., Barker, K. M., and Flynn, K. P. (1999). Identification and remediation of organic skin damage. *The 1999 AIChE Spring National Meeting, Houston, Texas. International Conference on Petroleum* and Gas Phase Behavior and Fouling, 14 – 18.

33. Rahman, P. A. (2017). Analysis of the mean time to data loss of nested disk arrays RAID-01 on basis of a specialized mathematical model. *IOP Conference Series: Materials Science and Engineering,* 177(1). https://doi.org/10.1088/1757-899X/177/1/012088

34. Ramey, H.J. (2013). Jr. Wellbore heat transmission. *Journal of Petroleum Technology* 14 (4), 872-875 https://doi.org/10.2118/96-PA

35. Rehan, M., Nizami, A.S., Taylan, O., Al-Sasi, B.O. and Demirbas, A., (2016). *Determination of wax content in crude oil. Petroleum Science and Technology, 34 (9), 799–804*. https://doi.org/10.1080/10916466.2016.1169287

36. Rogel, E., Roye, M., Vien, J., and Miao, T. (2015). Characterization of Asphaltene Fractions: Distribution, Chemical Characteristics, and Solubility Behavior. March. *Energy and Fuels, 29(4),* 2143-2152. *https://doi.org/10.1021/ef5026455*

37. Sumer, B.M. Lecture notes on turbulence (2007). *Technical University of Denmark*, available at: http://www.external.mek.dtu.dk/personal/bms/turb_bo- ok_update_30_6_04.pdf

38. Shirani, B., Nikazar, M., and Mousavi-Dehghani S. A. (2012). Prediction of asphaltene phase behavior in live oil with CPA equation of state. *Fuel*, 97, 89-96. https://doi.org/10.1016/j.fuel.2012.02.016

39. Shih, T.-H., Liou, W.W., Shabbir, A., Yang, Z., and Zhu J. (1995). A new k– eddy-viscosity model for high Reynolds number turbulent flows. Model development and validation. *Computers fluids*, № 24 (3), 227–238. https://doi.org/10.1016/0045-7930(94)00032-T

40. Soulgani, B. S., Rashtchian, D., Tohidi, B., and Jamialahmadi, M. (2010). A Novel Method for Mitigation of Asphaltene Deposition in the Wellstring*. Iranian Journal of Chemistry and Chemical Engineering*, 29 (2), 131-142. available at: http://www.ijcce.ac.ir/article_6709_9640cbd1410f6a223f64dbaba5cb9f0f.pdf

41. Sullivan, M., Smythe, E.J., Fukagawa, S., Hadrien Dumant., and Borman C., A (2020). Fast Measurement of Asphaltene Onset Pressure. *SPE Reservoir Evaluation and Engineering. 23(3).* https://doi.org/10.2118/199900-PA

42. Turbakov, M. S., Erofeev, A. A., and Lekomtsev, A.V. (2009). The Determination of Depth of the Beginning of Establishing of Asphaltene-Resin-Paraffin Deposits upon Operating the Oil-Producing Wells. *Geologiya, geofizika i razrabotka neftyanykh i gazovykh mestorozhdenij (Geology, Geophysics and Development of Oil and Gas Fields),* 10, 62-65.

43. Turbakov, M. S., Lekomtsev, A.V., and Erofeev, A. A. (2011). The Saturation Temperature of Oil with Paraffin for the Fields of the Upper Kama Region. *Neftyanoe khozyajstvo (Oil Industry)*, 8, 123-125.

44. Ustkachkintsev, E. N., and Melekhin, S. V. (2016). The Determination of Efficiency of Methods to Prevention of Asphalten-Resin-Paraffin Deposits. *Geologiya, geofizika i razrabotka neftyanykh i gazovykh mestorozhdenij (Geology, Geophysics and Development of Oil and Gas Fields),* 15 (18), 61-70.

45. Wang, W.D., Huang, Q.Y., Liu, Y.J., and Kamy Sepehrnoori. (2015). Experimental Study on Mechanisms of Wax Removal During Pipeline Pigging. *Presented at the SPE Annual Technical Conference and Exhibition, Houston, Texas, 28-30*

September.
https://doi.org/10.2118/174827-MS

46. Wilcox, David C (1998). Turbulence Modeling for CFD. *Second edition, Anaheim: DCW Industries*, 1998, pp. 174.
47. Yemelyanov, V. A., Yemelyanova, N. Y., Nedelkin, A. A., Glebov, N. B., and Tyapkin, D. A. (2019). Information system to determine the transported liquid iron weight. Paper presented at the *Proceedings of the 2019 IEEE Conference of Russian Young Researchers in Electrical and Electronic Engineering,* ElConRus 2019, 377-380. https://doi:10.1109/EIConRus.2019.8656693
48. Zhao, Y., Limb, D., and Zhu, X., (2017) A study of wax deposition in pipeline using thermal hydraulic model. *18th International Conference on Multiphase Production Technology, 7-9 June, Cannes, France.*
49. Zlobin, A. A. (2015). Experimental Studies of the Processes of Aggregation and Self-Assembly of Nanoparticles within Oil Disperse Systems. *Vestnik permskogo natsional'nogo issledovatel'skogo politekhnicheskogo universiteta. Geologiya. neftegazovoe i gornoe delo (The Bulletin of Perm National Research Polytechnic University. Geology. Oil, Gas and Mining*), 14 (15), 57-72.

(a) (b)

Figure 1. *Picture of ARPD Establishing onto the Surface of Deep-Pumping Equipment: (a) ARPD in Pipes; (b) Deposits onto Pump and Rods*

Source: the author

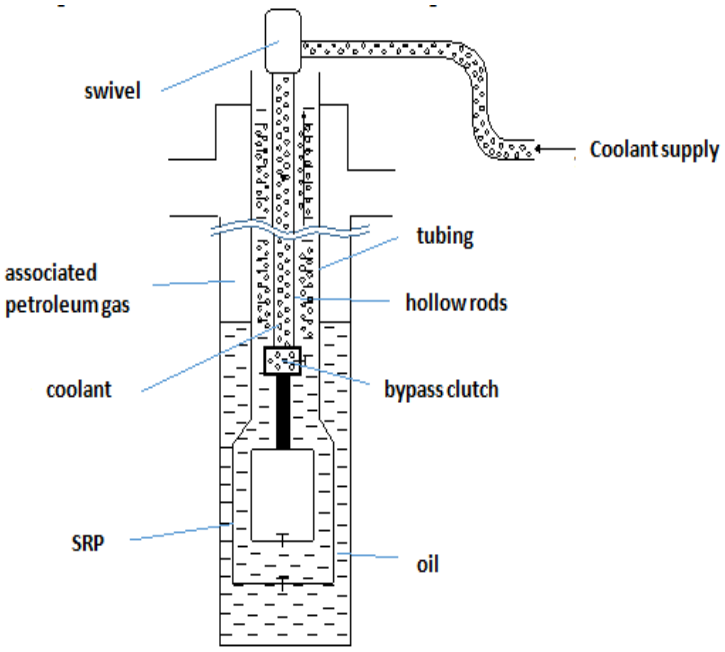

Figure 2. *Geometric Model of a Well Equipped with SRP with Hollow Rods. Source: The author.*

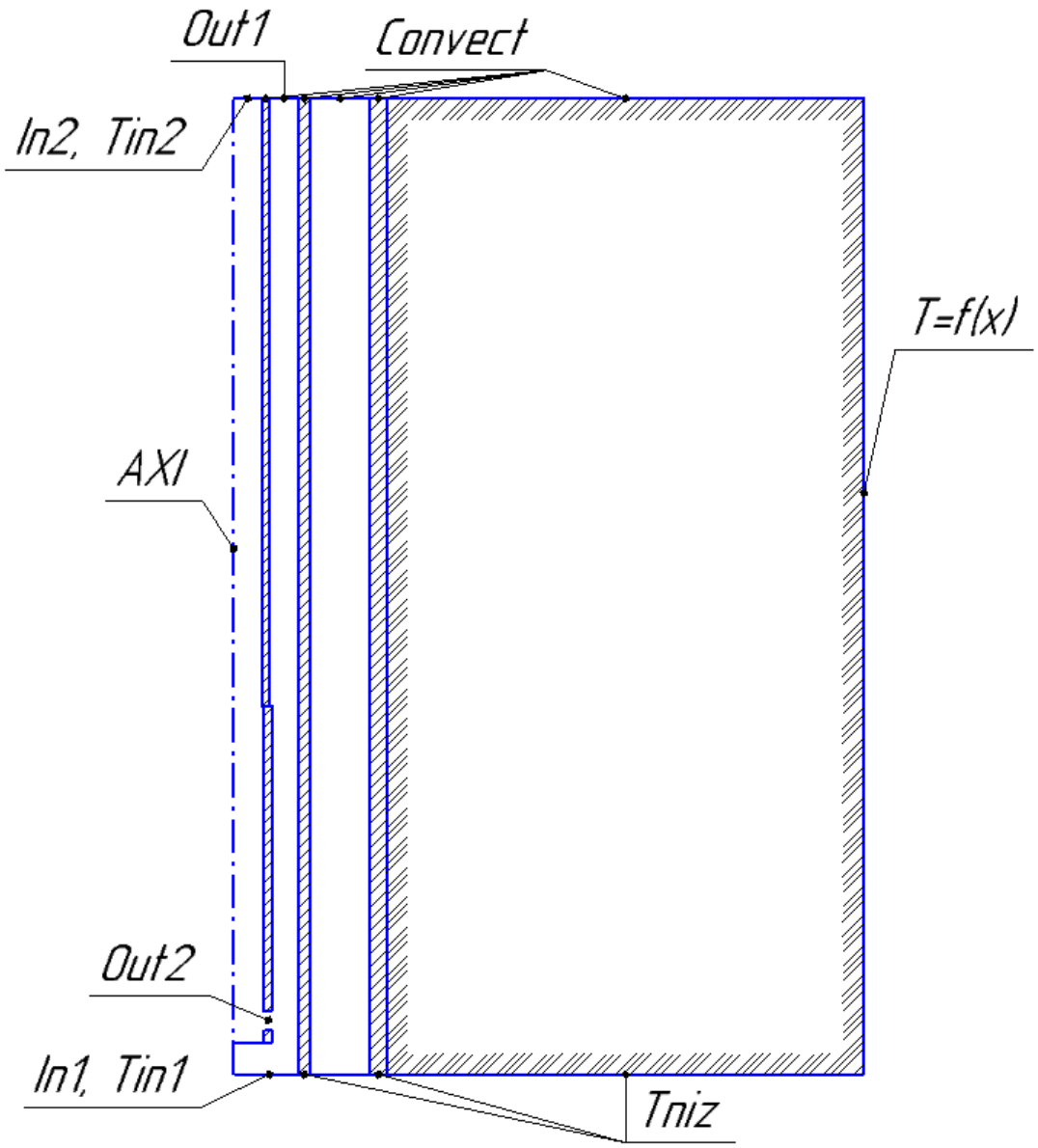

Figure 3. *Computational Domain with Boundary Conditions. Source: The author.*

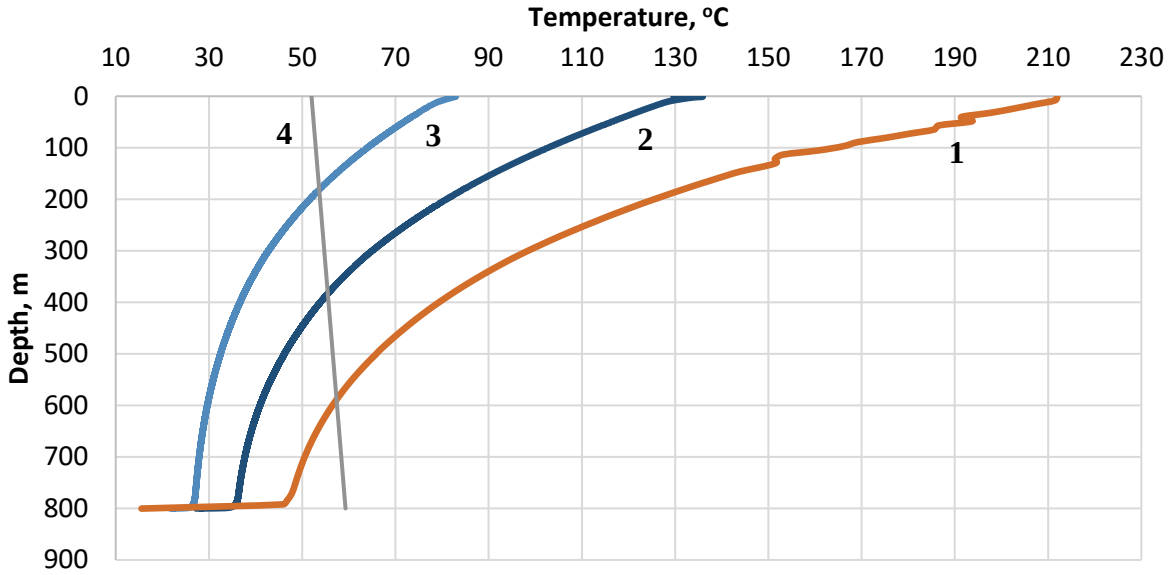

***Figure 4**. The Temperature Distribution onto the Inner Wall of the Tubing from the Depth under Different Temperatures of the Coolant. Dynamic Level – 0 m. Coolant - oil supplied with a flow rate of 150 m^3 / day and temperature: 1 – 300 ˚ C; 2 – 200 ˚ C; 3 – 120 ˚ C; 4 -the temperature of paraffin melting. Source: The author.*

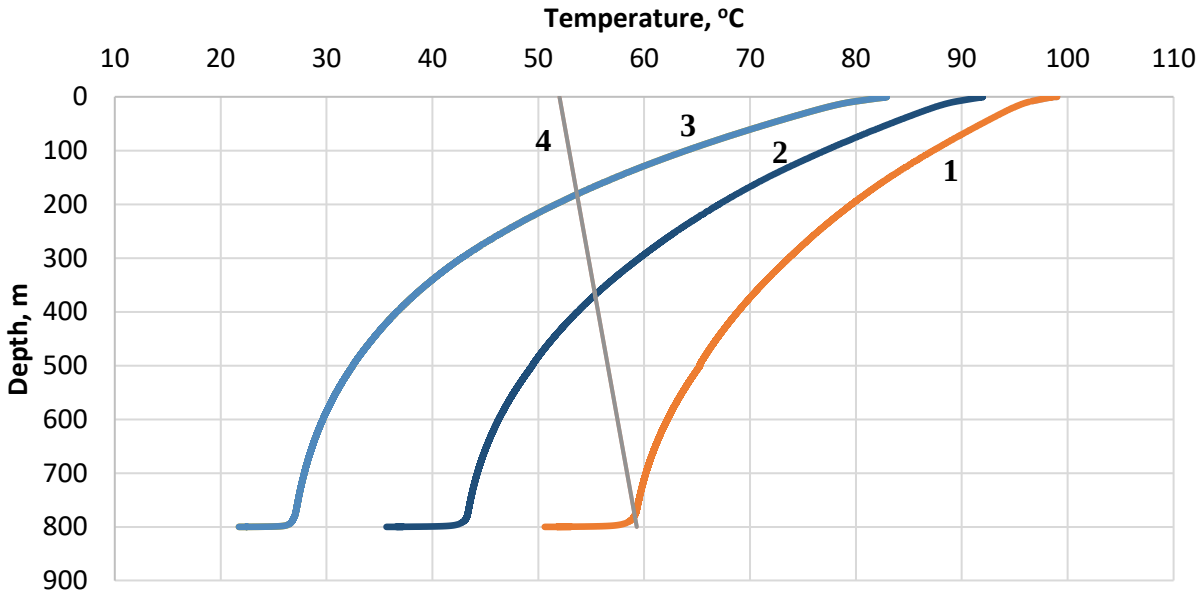

***Figure 5.** The temperature distribution onto the inner wall of the tubing from the depth under different coolant flow. Dynamic Level – 0 m. Coolant oil heated up to 120°C during injection consumption: 1- 300 m^3 / day; 2- 250 m^3/ day; 3- 150 m^3/ day; 4-the melting temperature of paraffin. Source: the author*

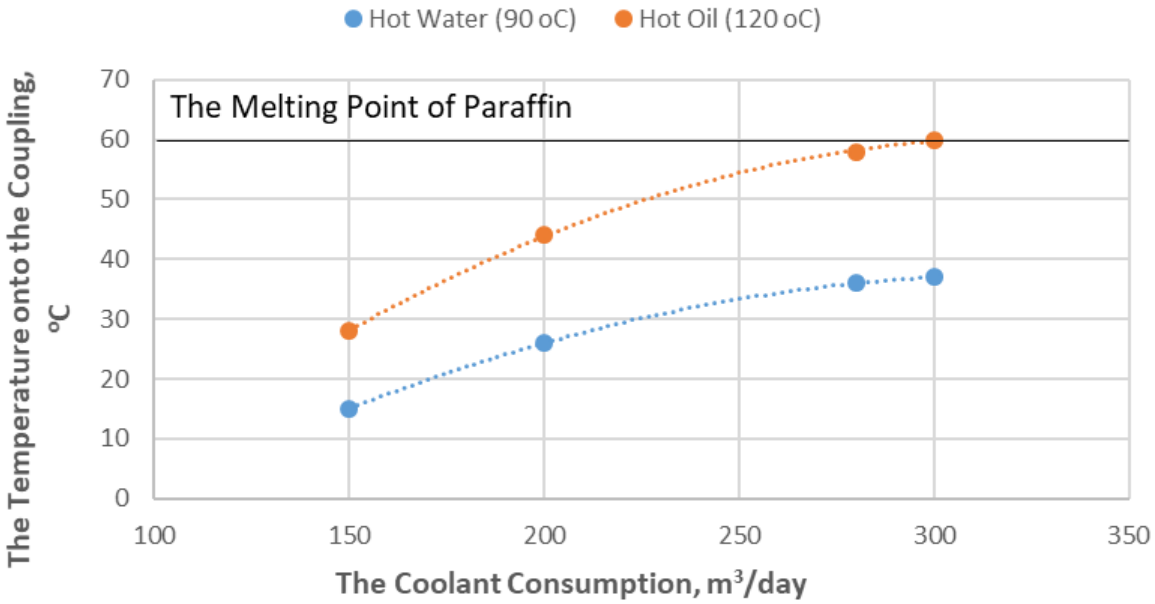

Figure 6. *The Dependence of the Downhole Production Temperature at the Coupling Level onto the Flow Rate and the Coolant Type. Source: the author*

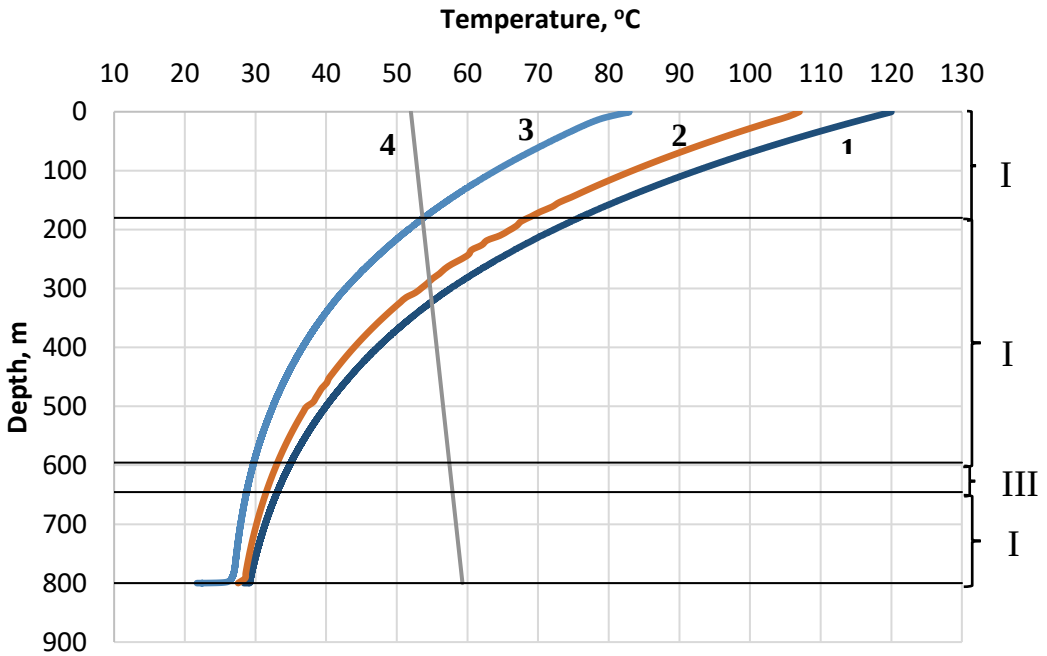

Figure 7. *The Temperature Distribution within the Well Depth. Coolant is the oil with its flow rate of 150 m³/day; within the annulus - oil, Hdyn= 0: 1 - is oil flow temperature in a hollow rod; 2- is hollow rod wall temperature; 3- is tubing wall temperature; 4 - is paraffin melting point. Source: the author*

Table 1. *Boundary conditions*

No.	Boundary condition	Specified parameter
1	AXI	Axis of symmetry
2	In1, Tin1	Plot of oil flow rates corresponding to the well production rate. Oil temperature at the coupling level equal to 15 °C
3	Out1	The boundary condition for the liquid outlet at the wellhead
4	In2, Tin2	Plot of coolant flow rates corresponding to a given flow rate. Heat carrier temperature equal to 90 °C for water and 120 °C for oil
5	Out2	The boundary condition for the release of the coolant from the coupling
6	Tniz	Temperature at the coupling level equal to 15 °C
7	Convect	Condition of natural convection on the surface
8	T=f(x)	Geothermal gradient equal to 0.2 °C / 10 m

Table 2. *The Properties of Materials and Media*

Material	Density ρ, kg / m^3	Heat capacity C, j/(kg·K)	Thermal Conductivity λ, W/(m·K)	Viscosity μ, MPa·s
Soil	1,900	1,680	1.82	-
Steel	8,030	502	16.27	-
Water	998.2	4,200	0.6	1
Oil	761.5	2,000	0.15	10
Associated Petroleum Gas	1.225	1,006	0.0242	0.0018

Table 3. *The Results of Calculation of Hydraulic Pressure Losses During Hot Water Washing*

No.	Characteristic	Hot Water onto the Rods Flow	
1	Rod Length, m	500	300
2	Inner Diametre of the Rod, mm	29	27
3	Consumption, m^3 / day	300	300
4	Kinematic Viscosity, mm^2 / s	0.326	0.326
	Result of Calculation		
1	Flow Rate, m / s	6.1	5.3
2	Reynolds number, un.	502,524	467,867
3	The Coefficient of Hydraulic Resistance, un.	0.0295	0.0290
4	Head Loss due to Friction, m	604	692
5	Friction Pressure Loss, MPa	6.0	6.9
6	Total Pressure Loss, MPa	**12.9**	

Table 4. *The Results of Calculation of Hydraulic Pressure Losses during Hot Oil Washing*

No.	Characteristic	Hot Oil onto the Rods Flow	
1	Rod Length, m	500	300
2	Inner Diametre of the Rod, mm	29	27
3	Consumption, m^3 / day	300	300
4	Kinematic Viscosity, mm^2 / s	1.71	1.71
	Result of Calculation		
1	Flow Rate, m / s	6.1	5.3
2	Reynolds number, un.	95,803	89,196
3	The Coefficient of Hydraulic Resistance, un.	0.0303	0.0299
4	Head Loss due to Friction, m	620	714
5	Friction Pressure Loss, MPa	6.2	7.1
6	Total Pressure Loss, MPa	**13.3**	

Table 5. *Probable Depth of ARPD Washing under Different H_{dyn} and a Type of the Heat Carrier*

Dynamic Level, m	Hot Oil (120˚C)	Hot water (90˚C)
0	645	360
300	698	427
500	above 800	500
800	above 800	596

Note: * Technological efficiency and probable depth of washing are provided at productivity of the unit (ADP, ADPM type) operated not below the second speed.